



Regulation of spinogenesis in mature Purkinje cells via mGluR/PCK-mediated phosphorylation of CaMKII β

Takeyuki Sugawara^a, Chihiro Hisatsune^{a,1}, Hiroyuki Miyamoto^{b,c}, Naoko Ogawa^a, and Katsuhiko Mikoshiba^{a,1}

^aLaboratory for Developmental Neurobiology, Brain Science Institute, RIKEN, Wako, Saitama 351-0198, Japan; ^bLaboratory for Neuronal Circuit Development, Brain Science Institute, RIKEN, Wako, Saitama 351-0198, Japan; and ^cPrecursory Research for Embryonic Science and Technology, Japan Science and Technology Agency, Kawaguchi, Saitama 332-0012, Japan

Edited by Solomon H. Snyder, Johns Hopkins University School of Medicine, Baltimore, MD, and approved May 18, 2017 (received for review October 19, 2016)

Dendritic spines of Purkinje cells form excitatory synapses with parallel fiber terminals, which are the primary sites for cerebellar synaptic plasticity. Nevertheless, how density and morphology of these spines are properly maintained in mature Purkinje cells is not well understood. Here we show an activity-dependent mechanism that represses excessive spine development in mature Purkinje cells. We found that CaMKII β promotes spine formation and elongation in Purkinje cells through its F-actin bundling activity. Importantly, activation of group I mGluR, but not AMPAR, triggers PKC-mediated phosphorylation of CaMKII β , which results in dissociation of the CaMKII β /F-actin complex. Defective function of the PKC-mediated CaMKII β phosphorylation promotes excess F-actin bundling and leads to abnormally numerous and elongated spines in mature IP₃R1-deficient Purkinje cells. Thus, our data suggest that phosphorylation of CaMKII β through the mGluR/IP₃R1/PKC signaling pathway represses excessive spine formation and elongation in mature Purkinje cells.

Purkinje cell | spine | phosphorylation | CaMKII | PKC

In the cerebellum, Purkinje cells are the sole output from the neural circuit of the cerebellar cortex, and integrate numerous synaptic inputs (1). Spines along the distal dendrites of Purkinje cells form excitatory synapses with parallel fiber terminals, which are the primary sites of cerebellar synaptic plasticity (1, 2). Spine density and morphology of Purkinje cells change significantly during development (3, 4), and morphological abnormalities of spines are closely associated with many neurological disorders (5–7). Recent studies also demonstrated that some forms of training for cerebellar motor learning results in altered spine density in Purkinje cells (8, 9). Thus, maintenance of proper spine density and morphology of Purkinje cells is a critical aspect of cerebellar functions. However, the precise molecular mechanisms that maintain Purkinje cell spine density and morphology remain unclear.

The actin filaments are a major structural element of the regulation of dendritic spine formation and morphology of neurons (10, 11). The actin dynamics in spines are regulated by many actin-related molecules including Ca²⁺/calmodulin-dependent protein kinase II (CaMKII) (12), which is one of the most abundant proteins in the brain (13). Among CaMKII isoforms (α , β , γ , and δ), CaMKII β possesses a specific F-actin binding domain (14) and plays an important role for regulating dendritic spine structure in hippocampal neurons. It is reported that suppression of CaMKII β expression leads to reduced spine formation, and conversely, overexpression of CaMKII β increases synapse number and motility of filopodia in hippocampal neurons (15, 16). The effect of CaMKII β on maintaining mature spine structure requires its F-actin binding and bundling activity, but not its kinase activity (17). In addition, a recent study reported that in hippocampal neurons, activation of CaMKII β by postsynaptic Ca²⁺ influx through the NMDA receptor and resultant autophosphorylation within the F-actin binding domain induces detachment of CaMKII β from F-actin in spines, which influences functional and structural plasticity (18). However, the precise regulatory mechanisms governing the association of CaMKII β with F-actin are not fully

understood. In addition, although CaMKII β is predominantly expressed in the cerebellum (19, 20), how CaMKII β contributes to regulating the spine morphology of cerebellar neurons remains largely unknown.

In this study, we examined whether/how CaMKII β regulates spine density and morphology in Purkinje cells. We found that overexpression of CaMKII β promotes spine formation and elongation in Purkinje cells by accelerating F-actin bundling. In addition, we found that CaMKII β at Ser315 (S315) is phosphorylated by Ca²⁺-dependent isoforms of protein kinase C (PKC) in Purkinje cells, and that the phosphorylation is triggered by group I metabotropic glutamate receptor (mGluR)-type 1 inositol 1,4,5-trisphosphate receptor (IP₃R1) signaling, but not by postsynaptic Ca²⁺ influx. The phosphorylation of CaMKII β at S315 interferes with its F-actin binding and bundling activity, resulting in suppression of CaMKII β -mediated excess spine formation and elongation of Purkinje cells. We also found that PKC-mediated CaMKII β phosphorylation is impaired in IP₃R1-deficient Purkinje cells that exhibit an abnormally increased number of spines. These findings suggest that CaMKII β controls spine morphology in Purkinje cells under control of the mGluR1/IP₃R1/PKC signaling pathway.

Results

CaMKII β Controls Spine Morphology and Formation in Purkinje Cells.

Given the implication that CaMKII β regulates the dendritic spine morphology of hippocampal neurons through its F-actin bundling and stabilizing activity (17) and that CaMKII β highly expresses in the cerebellum (19, 20), we examined whether CaMKII β also contributes to the spine morphology of Purkinje cells. For this analysis, we

Significance

The cerebellar cortex, and its sole output, Purkinje cells, is essential for motor coordination and learning. Dendritic spines of Purkinje cells are the primary sites of cerebellar synaptic plasticity. Therefore, maintenance of spine structure of mature Purkinje cells is a critical aspect of cerebellar functions, but the underlying mechanisms remain unclear. Here we described an activity-dependent regulatory mechanism of spines in Purkinje cells. We found that F-actin cross-linking activity of Ca²⁺/calmodulin-dependent protein kinase II β isoform is controlled by protein kinase C-mediated phosphorylation, which is triggered by group I metabotropic glutamate receptor signaling. Defective function of the phosphorylation leads to excess spine development in mature Purkinje cells. Our findings revealed a mechanism for proper maintenance of cerebellar Purkinje cell spines.

Author contributions: T.S., C.H., and K.M. designed research; T.S., H.M., and N.O. performed research; T.S. analyzed data; and T.S. and C.H. wrote the paper.

The authors declare no conflict of interest.

This article is a PNAS Direct Submission.

¹To whom correspondence may be addressed. Email: mikosiba@brain.riken.jp or chihiro@brain.riken.jp.

This article contains supporting information online at www.pnas.org/lookup/suppl/doi:10.1073/pnas.1617270114/-DCSupplemental.

biologically coexpressed HA-CaMKII β and EGFP in Purkinje cells of cerebellar slices from mice at 14–17 d after birth and subsequently visualized the spine morphology after 2 d. We found that overexpression of the wild-type form of HA-tagged CaMKII β (HA-CaMKII β -WT) significantly increased the spine density and spine length in Purkinje cells (Fig. 1A and B). In contrast, the width of the spine head was not apparently changed by CaMKII β . The kinase activity was not essential for the spine regulation, because kinase-dead mutant (CaMKII β -K43M) also increased the spine density and length of Purkinje cells, similarly to CaMKII β -WT (Fig. 1A and B). These results suggest that CaMKII β controls spine density and morphology of Purkinje cells independently of kinase activity similarly to mechanisms within hippocampal neurons (15, 16).

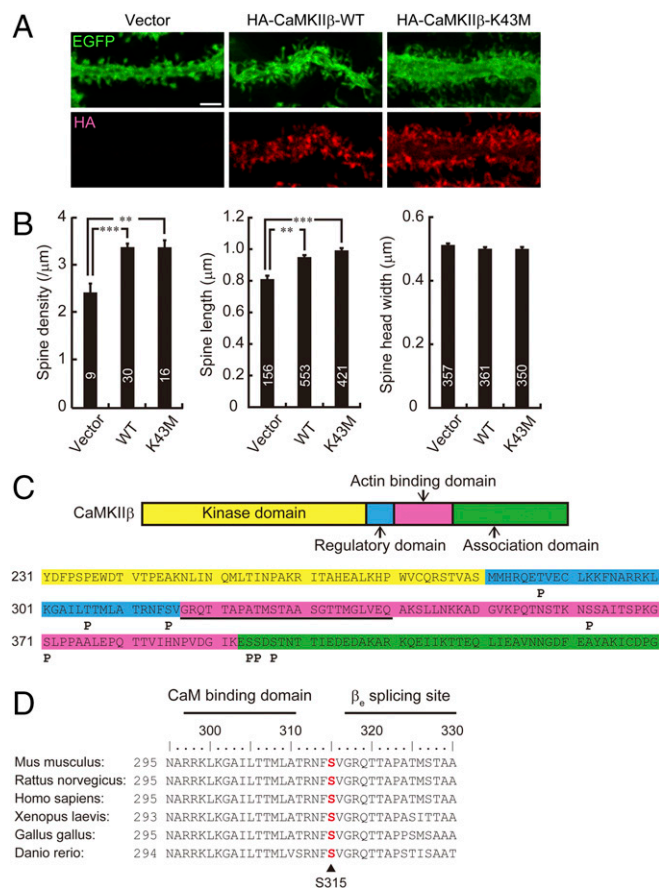


Fig. 1. CaMKII β controls spine morphology and is phosphorylated at S315 in Purkinje cells. (A) Effects of overexpression of WT or K43M mutant form of HA-tagged CaMKII β on Purkinje cell dendritic spine morphology in cerebellar slice cultures. Cerebellar slices were subjected to biolistic cotransfection with HA-CaMKII β and EGFP, cultured for 2 d, and immunostained with anti-EGFP and HA antibodies. Representative images of distal dendrites of Purkinje cells are shown. (Scale bar, 2 μ m.) (B) Quantitative analysis of spine density along distal dendrites (Left), spine length (Center), and spine head width (Right) of EGFP⁺ Purkinje cells in A. ****** P < 0.01, ******* P < 0.0001, one-way ANOVA with Bonferroni's test for multiple comparisons. (C) Summary of in vivo phosphorylation sites of CaMKII β in Purkinje cells. Phosphorylation sites are depicted as "P." The critical F-actin binding region (317–340 aa) is underlined. Detailed information is provided in Fig. S1. (D) Conservation of S315 (in red) in CaMKII β among species. Calmodulin (CaM) binding domain and β_e splicing site of CaMKII β are also shown. Each amino acid sequence is from accession numbers NP_031621.3 (*Mus musculus*), NP_068507.2 (*Rattus norvegicus*), NP_742075.1 (*Homo sapiens*), NP_001084063.1 (*Xenopus laevis*), NP_989625.1 (*Gallus gallus*), or XP_009303979.1 (*Danio rerio*). The numbers of neurons or spines are indicated in each graph.

CaMKII β Is Phosphorylated at Ser315 in Purkinje Cells. It has been reported that autophosphorylation of serine (Ser) and threonine (Thr) residues within the actin-binding domain of CaMKII β mediates structural plasticity of spines through the F-actin regulation in hippocampal neurons (17, 18). Therefore, we examined whether CaMKII β is phosphorylated in Purkinje cells in vivo. Because CaMKII β is expressed not only in Purkinje cells but also in other cerebellar neurons (21, 22), we coimmunoprecipitated CaMKII β as an immunocomplex of CaMKII α , an isoform selectively expressed in Purkinje cells, and examined the phosphorylation state of CaMKII β of Purkinje cells by mass-spectrometric phosphopeptide mapping. We found that S315, which resides near the critical F-actin binding region (317–340 aa) (Fig. 1C and Fig. S1) and is conserved across various species (Fig. 1D), was phosphorylated in Purkinje cells in vivo. In our analysis with the cerebellar samples, we could not detect the previously reported phosphorylated residues that reside within the critical F-actin binding region (317–340 aa) of CaMKII β from hippocampal neurons (18, 23) (Fig. 1C). Therefore, we focused on the S315 phosphorylation of CaMKII β in later studies.

Activation of Group I mGluR Leads to Phosphorylation of CaMKII β at S315 in Purkinje Cells. To monitor the phosphorylation state of CaMKII β at S315 of Purkinje cells, we first developed an antibody that specifically recognizes phosphorylated CaMKII β at S315 (pS315). The specificity of the pS315-CaMKII β antibody was confirmed by immunoblotting of the lysates of HeLa cells transiently expressing WT or the phosphorylation-site mutant (S315A) form of CaMKII β . As shown in Fig. 2A, the pS315-CaMKII β antibody recognized CaMKII β -WT, but not S315A mutant. In addition, treatment of the cells with okadaic acid (OA), an inhibitor of the Ser/Thr protein phosphatase, significantly enhanced the signal of CaMKII β -WT (Fig. 2A). Thr287 (T287) was phosphorylated in both CaMKII β -WT and -S315A mutant, and the phosphorylation is enhanced after OA treatment, suggesting that the S315 antibody does not recognize other phosphorylation sites of CaMKII β . The specificity of the antibody was also confirmed by immunocytochemical analysis (Fig. 2B). These results suggested that the pS315-CaMKII β antibody specifically recognizes CaMKII β phosphorylated at S315.

We next assessed whether synaptic activity affects the phosphorylation level of S315-CaMKII β in cultured cerebellar neurons. We found that application of glutamate, the principal neurotransmitter at excitatory synapses, significantly increased the phosphorylation level of CaMKII β at S315 in cerebellar neurons (Fig. 2C). Because CaMKII β is expressed in both cerebellar granule cells and Purkinje cells (21, 22), we further performed immunocytochemical analysis to see whether the enhanced phosphorylation of S315-CaMKII β occurred in Purkinje cells. We found that glutamate application significantly increased the phosphorylation level of S315-CaMKII β in cultured Purkinje cells, especially at the spines (Fig. 2D).

To examine the signal pathway for triggering phospho-S315 CaMKII β elevation in Purkinje cells upon glutamate stimulation, we applied a group I mGluR agonist, dihydroxyphenylglycine (DHPG), to the culture. We found that DHPG also increased the phosphorylation level of S315-CaMKII β in Purkinje cells (Fig. 2E). In contrast, neither α -amino-3-hydroxy-5-methyl-4-isoxazolepropionic acid (AMPA)-type ionotropic glutamate receptor (AMPA) activation (AMPA application) nor depolarization (high K^+ stimulation) efficiently increased the phosphorylation level of S315-CaMKII β in Purkinje cells, although they did in other types of cerebellar neurons, most frequently granule cells (Fig. 2E). Because the influx of Ca^{2+} through voltage-dependent Ca^{2+} channels activates CaMKII in Purkinje cells (24), phosphorylation at S315 of CaMKII β was not due to autophosphorylation by CaMKII itself in Purkinje cells. We further confirmed that both of the

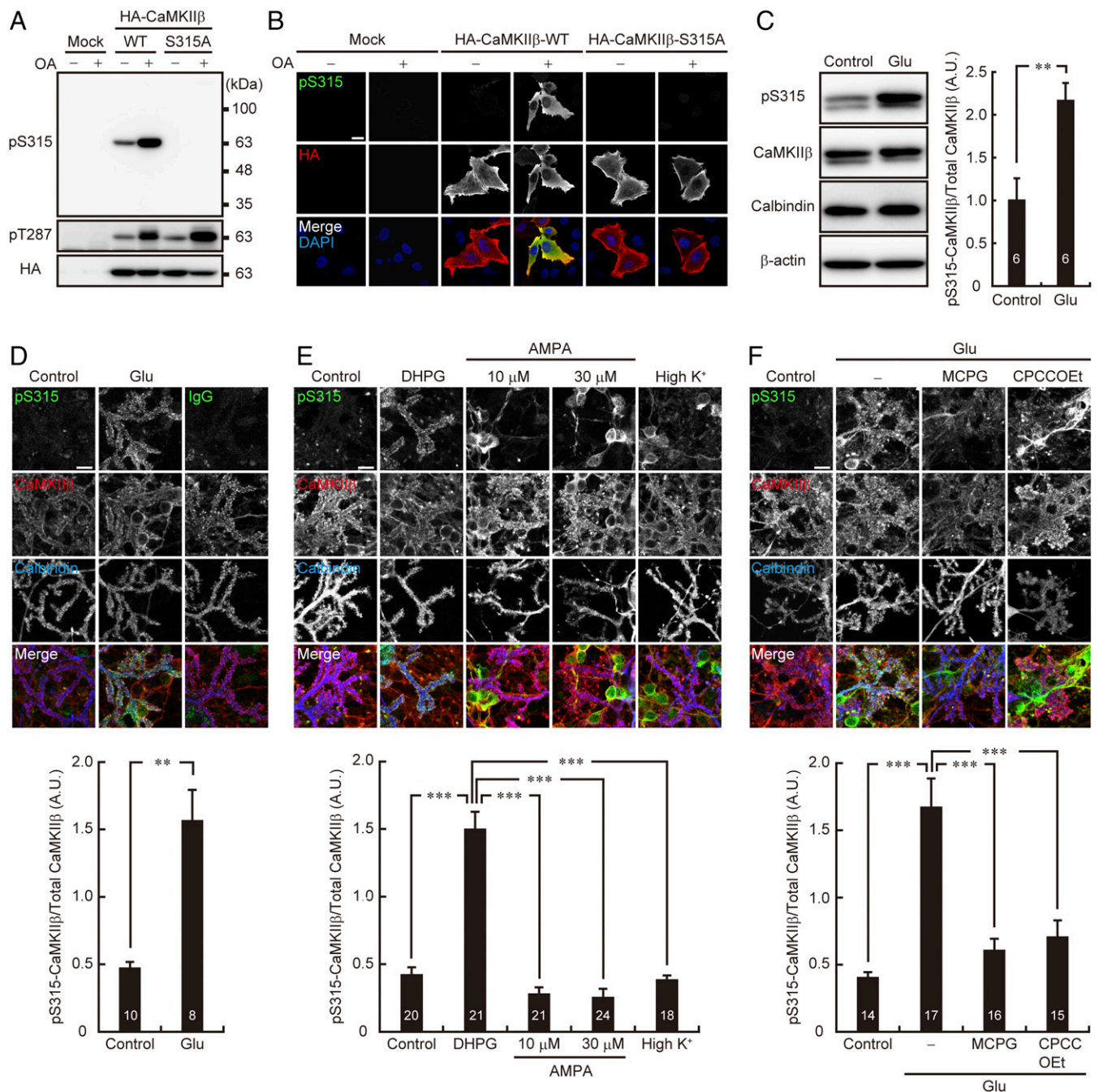


Fig. 2. Synaptic activity increases CaMKII β phosphorylation at S315 in Purkinje cells via group I mGluR signaling. (A and B) The specificity of the phospho-S315 (pS315) CaMKII β antibody. WT and S315A mutant form of HA-tagged CaMKII β overexpressed in HeLa cells were subjected to immunoblotting (A) or immunocytochemical analysis (B) with the indicated antibodies. OA: 1 μ M okadaic acid treatment for 30 min. (Scale bar, 20 μ m.) (C) CaMKII β phosphorylation at S315 in cultured cerebellar cells before (Control) and after (Glu) 10 μ M glutamate stimulation for 10 min. The treated cells were subjected to immunoblot analysis with indicated antibodies (Left). Band intensities of CaMKII β phosphorylated at S315 (pS315) and total CaMKII β were quantified, and the phosphorylation level was calculated by dividing the band intensity of pS315-CaMKII β by that of total CaMKII β (Right). **** P < 0.01**, Student's *t* test. (D–F) Immunocytochemistry of CaMKII β phosphorylation at S315 in cultured Purkinje cells upon pharmacological stimulation of synaptic activity. Primary cultured cerebellar cells were treated with 10 μ M glutamate (Glu) for 10 min (D), 100 μ M DHPG, or 10 or 30 μ M AMPA for 10 min, or 55 mM KCl (high K^+) for 2 min (E), and 10 μ M Glu for 10 min in the presence or absence of 1 mM MCPG or 100 μ M CPCCOEt (F). The treated cells were immunostained with the indicated antibodies. Purkinje cell distal dendritic areas are shown. (Scale bars, 10 μ m.) Quantification of the phosphorylation level of CaMKII β at S315 in Purkinje cells is shown (Lower). Fluorescent intensities of CaMKII β phosphorylated at S315 (pS315) and total CaMKII β in the distal dendritic area of Purkinje cells identified with Calbindin staining were quantified, and the phosphorylation level was calculated by dividing the immunoreactivity of pS315-CaMKII β by that of total CaMKII β . (D) **** P < 0.01**, Mann–Whitney *U* test. (E) ***** P < 0.0001**, one-way ANOVA with Bonferroni's test for multiple comparisons. (F) ***** P < 0.0001**, one-way ANOVA with Bonferroni's test for multiple comparisons. The numbers of experiments (C) or neurons (D–F) are indicated in each graph.

mGluR inhibitors, (+)- α -methyl-4-carboxyphenylglycine (MCPG) and 7-(hydroxyimino)cyclopropa[b]chromen-1 α -carboxylate ethyl ester (CPCCOEt), blocked glutamate-induced S315 phosphorylation

of CaMKII β in Purkinje cells (Fig. 2F). These results suggested that synaptic activity modulates the phosphorylation state of S315-CaMKII β via the mGluR signal pathway in Purkinje cells.

mGluR Stimulation Increases Phosphorylation of CaMKII β at S315 Through IP₃R1- PKC Signaling in Purkinje Cells. Because mGluR activation produces IP₃ and leads to subsequent Ca²⁺ release from intracellular Ca²⁺ stores via IP₃Rs, and because IP₃R1 is a critical regulator of Purkinje cell spines in the mature cerebellum in vivo (25, 26), we subsequently examined the pS315-CaMKII β level in IP₃R1-deficient Purkinje cells. We prepared cultured cerebellar neurons from *Itp1*^{+/+} and *Itp1*^{-/-} mice and assessed the phosphorylation level of S315-CaMKII β in Purkinje cells following mGluR stimulation. In cultured *Itp1*^{+/+} Purkinje cells, DHPG stimulation increased the immunosignal of S315-CaMKII β especially at dendritic spines (Fig. 3A). In contrast, DHPG application failed to increase the phosphorylation level of S315-CaMKII β in

cultured *Itp1*^{-/-} Purkinje cells (Fig. 3B). The marked increase of the phosphorylation level of CaMKII β at S315 was also observed in *Itp1*^{flx/flx}, but not in Purkinje cell-specific conditional knockout (*L7-Cre;Itp1*^{flx/flx}) Purkinje cells, of acute cerebellar slices, when we applied DHPG to the slices (Fig. 3C).

It is widely believed that Ca²⁺ release via IP₃R1 is a critical event for activation of Ca²⁺-dependent isoforms of PKC (α , β , and γ), which is necessary for induction of cerebellar long-term depression (LTD) (25, 27). Therefore, we further examined involvement of PKC in S315-CaMKII β phosphorylation. We found that preincubation with Go6976, a selective inhibitor for Ca²⁺-dependent PKC isoforms (28), abolished the DHPG-induced elevation of pS315-CaMKII β level in *Itp1*^{+/+} Purkinje cells (Fig. 3A). Furthermore, direct

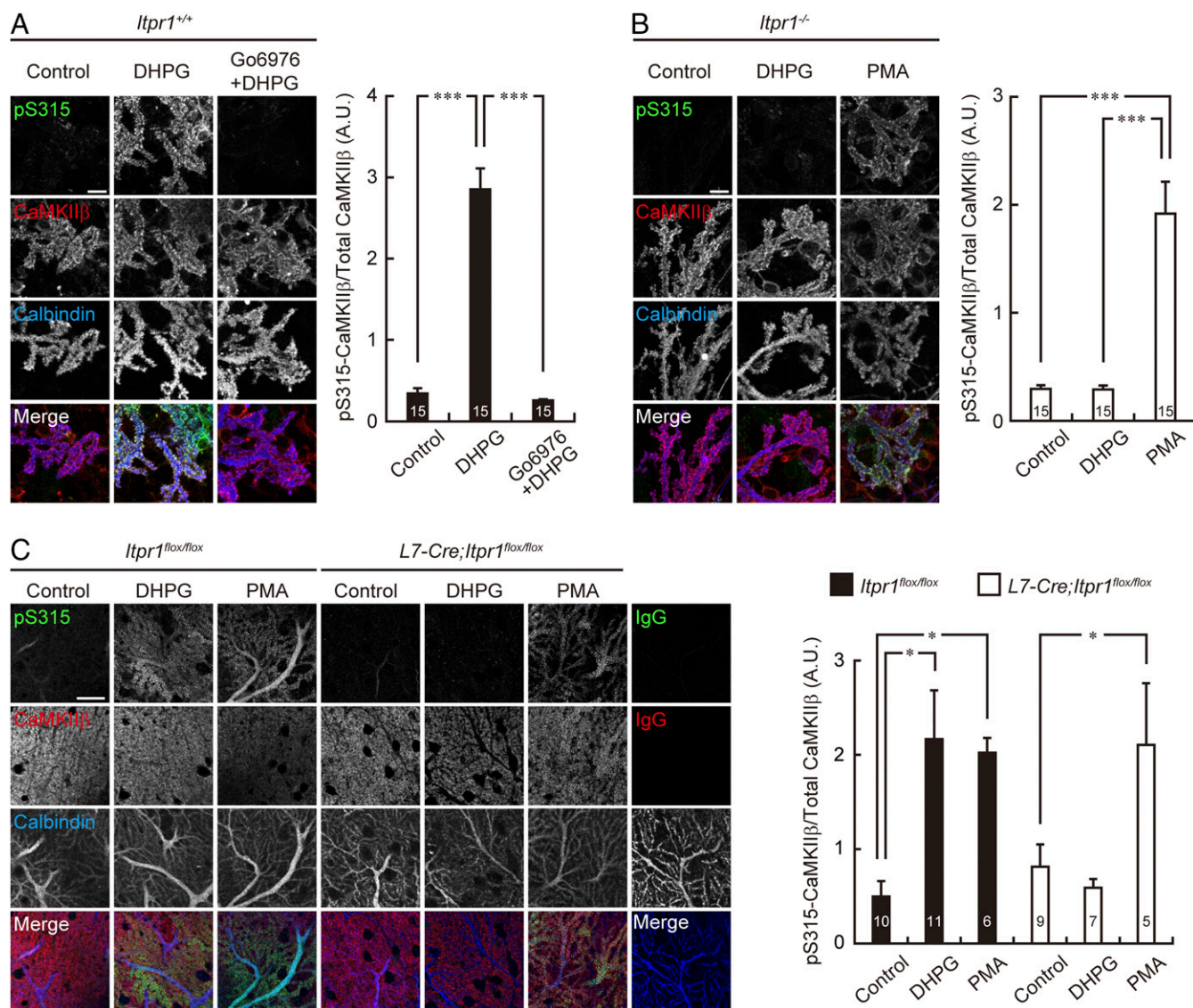


Fig. 3. mGluR stimulation increases CaMKII β phosphorylation at S315 through IP₃R1/PKC signaling. (A and B) Immunostaining of PKC-mediated phosphorylation of CaMKII β at S315 upon mGluR stimulation in cultured *Itp1*^{+/+} and *Itp1*^{-/-} Purkinje cells. Primary cultured cerebellar cells from *Itp1*^{+/+} mice were treated with 100 μ M DHPG for 10 min in the presence or absence of 5 μ M Go6976 (A), and cells from *Itp1*^{-/-} mice were treated with 100 μ M DHPG or 0.4 μ M PMA for 10 min (B). Treated cells were immunostained with the antibodies indicated. Purkinje cell distal dendritic areas are shown. (Scale bars, 10 μ m.) Quantification of the phosphorylation level of CaMKII β at S315 in the distal dendritic area of Purkinje cells are shown at Right. *** P < 0.0001, one-way ANOVA with Bonferroni's test for multiple comparisons. (C) Immunohistochemistry of S315 phosphorylation of CaMKII β of Purkinje cells in acute cerebellar slices prepared from *Itp1*^{flx/flx} and *L7-Cre;Itp1*^{flx/flx} mice. The slices were treated with 100 μ M DHPG for 5 min or 0.4 μ M PMA for 15 min, resectioned, and immunostained with the indicated antibodies. Distal dendritic areas of Purkinje cells are shown. (Scale bar, 20 μ m.) Quantification of the phosphorylation level of CaMKII β at S315 in Purkinje cells is shown at Right. * P < 0.05, one-way ANOVA with Dunnett's multiple-comparison post hoc test compared with control within each genotype. The numbers of neurons (A and B) and sections (C) are indicated in each graph.

activation of PKC with phorbol 12-myristate 13-acetate (PMA) increased the phosphorylation level of S315-CaMKII β in cultured *Itp1*^{-/-} Purkinje cells (Fig. 3B) and also in both *Itp1*^{flox/flox} and *L7-Cre;Itp1*^{flox/flox} Purkinje cells of acute cerebellar slices (Fig. 3C).

We also found that although PKC γ , which is an especially abundant isoform of PKCs in Purkinje cells (29), localized along plasma membrane in the *Itp1*^{flox/flox} Purkinje cell dendrites, such a restricted distribution of PKC γ at the plasma membrane was diminished in most of *L7-Cre;Itp1*^{flox/flox} Purkinje cell dendrites (Fig. S2 A–D). In addition, the phosphorylation rate of myristoylated alanine-rich C-kinase substrate (MARCKS), a substrate of PKC (30, 31), was much lower in *L7-Cre;Itp1*^{flox/flox} Purkinje cells than in *Itp1*^{flox/flox} cells (Fig. S2E), suggesting that PKC γ activation was impaired in IP₃R1-deficient Purkinje cells. These results suggested that the mGluR stimulation increased S315 phosphorylation of CaMKII β via IP₃R1/Ca²⁺-dependent PKC signal pathway in Purkinje cells.

PKC γ Directly Phosphorylates CaMKII β at S315. To examine whether PKC γ directly phosphorylates CaMKII β at S315, we performed an in vitro kinase assay of PKC γ using CaMKII β as a substrate. As shown in Fig. 4A, PKC γ directly phosphorylated GST-CaMKII β (272–407 aa) in vitro. In addition, when we coexpressed PKC γ and CaMKII β in HeLa cells and treated the cells with PMA, immunosignals of pS315-CaMKII β were clearly detected. However, those signals were abolished in cells expressing the nonphosphorylatable S315A mutant form of CaMKII β with PKC γ (Fig. 4B and C). These results suggested that PKC γ directly phosphorylates CaMKII β at S315 in living cells.

CaMKII β Phosphorylation at S315 Decreases Its F-Actin Binding and Bundling Activity. Because S315 localizes near the β_c splicing site, which is a critical regulatory region for F-actin binding of CaMKII β (18, 23) (Fig. 1D), we next examined the effect of the S315 phosphorylation of CaMKII β on its F-actin bundling activity. For this analysis, we prepared purified CaMKII β protein having phosphomimetic S315D mutation and assessed its F-actin bundling activity by in vitro F-actin cosedimentation assay. As shown in Fig. 5A, F-actin was well coprecipitated with CaMKII β -WT in a dose-dependent manner. In contrast, CaMKII β -S315D showed marked decrease of the bundled F-actin compared with CaMKII β -WT.

We also performed biochemical assessment of the CaMKII β /F-actin interaction in HeLa cells by detergent-extraction protocol (32, 33). As shown in Fig. 5B, detergent-insoluble actin-enrich pellet contains much less HA-CaMKII β -S315D than it does HA-CaMKII β -WT. Conversely, a greater amount of CaMKII β -S315D was detected in the soluble fraction than CaMKII β -WT.

Moreover, CaMKII β -S315D but not CaMKII β -S315A mutant showed decreased colocalization signals with F-actin compared with CaMKII β -WT in HeLa cells (Fig. 5C). Similar results were obtained in a kinase dead form of CaMKII β -S315D mutant (Fig. S3), neglecting a possible involvement of other autophosphorylated residues in the event. Furthermore, when we overexpressed CaMKII β -WT or S315A with PKC γ in HeLa cells, CaMKII β -WT, but not S315A, immunosignal was detached from F-actin signals after PMA application (Fig. 5D). These data suggested that PKC γ specifically phosphorylated S315 of CaMKII β and regulated the CaMKII β /F-actin association.

Purkinje Cell Spines Are Regulated by Phosphorylation State of CaMKII β at S315. Next, we examined whether the S315 phosphorylation state of CaMKII β affects the spine morphology of Purkinje cells. To minimize the effect of endogenous CaMKII β , we used a short hairpin RNA (shRNA), which specifically and efficiently downregulates CaMKII β (Fig. S4), and replaced the endogenous protein with exogenous HA-tagged CaMKII β . As shown in Fig. 6A–D, shRNA against CaMKII β did not affect the spine density and morphology of Purkinje cells, which is consistent with previous studies (20, 34). We found that replacement of endogenous CaMKII β with

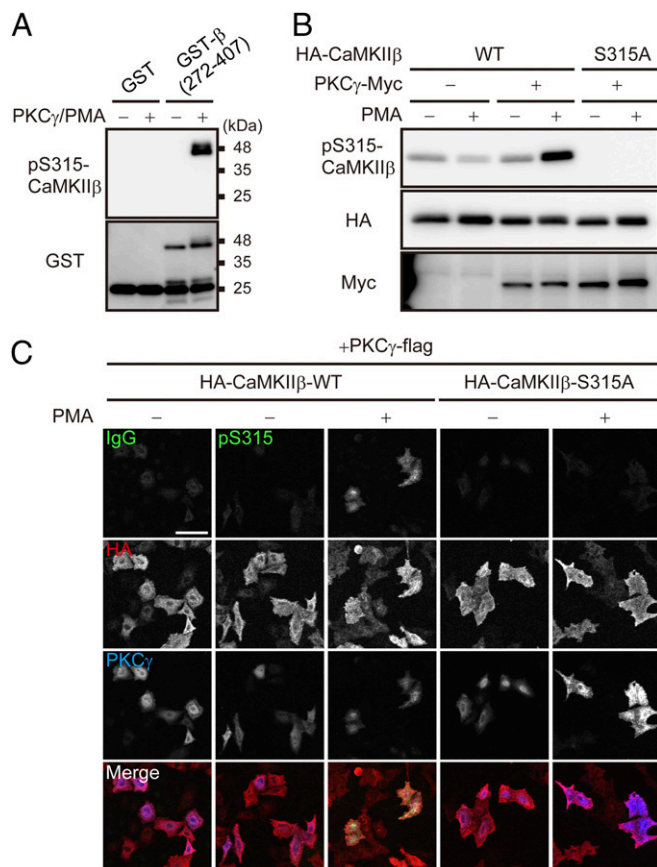


Fig. 4. PKC γ directly phosphorylates CaMKII β at S315. (A) Detection of PKC γ -mediated phosphorylation of GST-CaMKII β (GST- β) (272–407 aa) with anti-pS315-CaMKII β antibody. GST or GST- β (272–407 aa) were phosphorylated by PKC γ in vitro and subjected to immunoblot analysis. (B) Immunoblot analysis of WT and S315A mutant form of HA-tagged CaMKII β that were cotransfected with PKC γ -Myc in HeLa cells. Transfected cells were treated with or without 100 nM PMA for 30 min and subjected to immunoblot analysis with the indicated antibodies. (C) Immunocytochemistry of S315 phosphorylation of the WT or S315A mutant form of HA-CaMKII β cotransfected with PKC γ -flag in HeLa cells. The cells were treated with (+) or without (-) PMA and stained with the indicated antibodies. (Scale bar, 100 μ m.)

CaMKII β -S315A, but not with CaMKII β -S315D, significantly increased the spine density and length in Purkinje cells (Fig. 6A–C), as similar to overexpression of CaMKII β -WT (Fig. 1A and B). The kinase activity of CaMKII β was not involved in the pS315-CaMKII β -dependent regulation of spine morphology, because the double mutant CaMKII β -K43M/S315A but not K43M/S315D also increased spine density and length of Purkinje cells (Fig. 6A–C). The spine head width was not affected by any of the transfected Purkinje cells (Fig. 6D). These spine morphological changes were apparent in the distal dendritic region, but not in the proximal region of Purkinje cells (Fig. S5). These data suggested that the phosphorylation state of CaMKII β at S315 is critical for controlling spine density and morphology in Purkinje cells, especially along the distal dendritic region.

Inhibition of CaMKII β /F-Actin Interaction Ameliorates Spine Abnormality in IP₃R1-Deficient Purkinje Cells. Because the spine abnormalities of Purkinje cells expressing CaMKII β -S315A resembled those of IP₃R1-deficient Purkinje cells, which exhibit increased spine density and length but not head width specifically at the distal dendritic region (26), and because activity-dependent increase of CaMKII β -S315 phosphorylation was diminished in IP₃R1-deficient Purkinje cells (Fig. 3), we hypothesized that excess F-actin bundling by CaMKII β due to defect of S315 phosphorylation

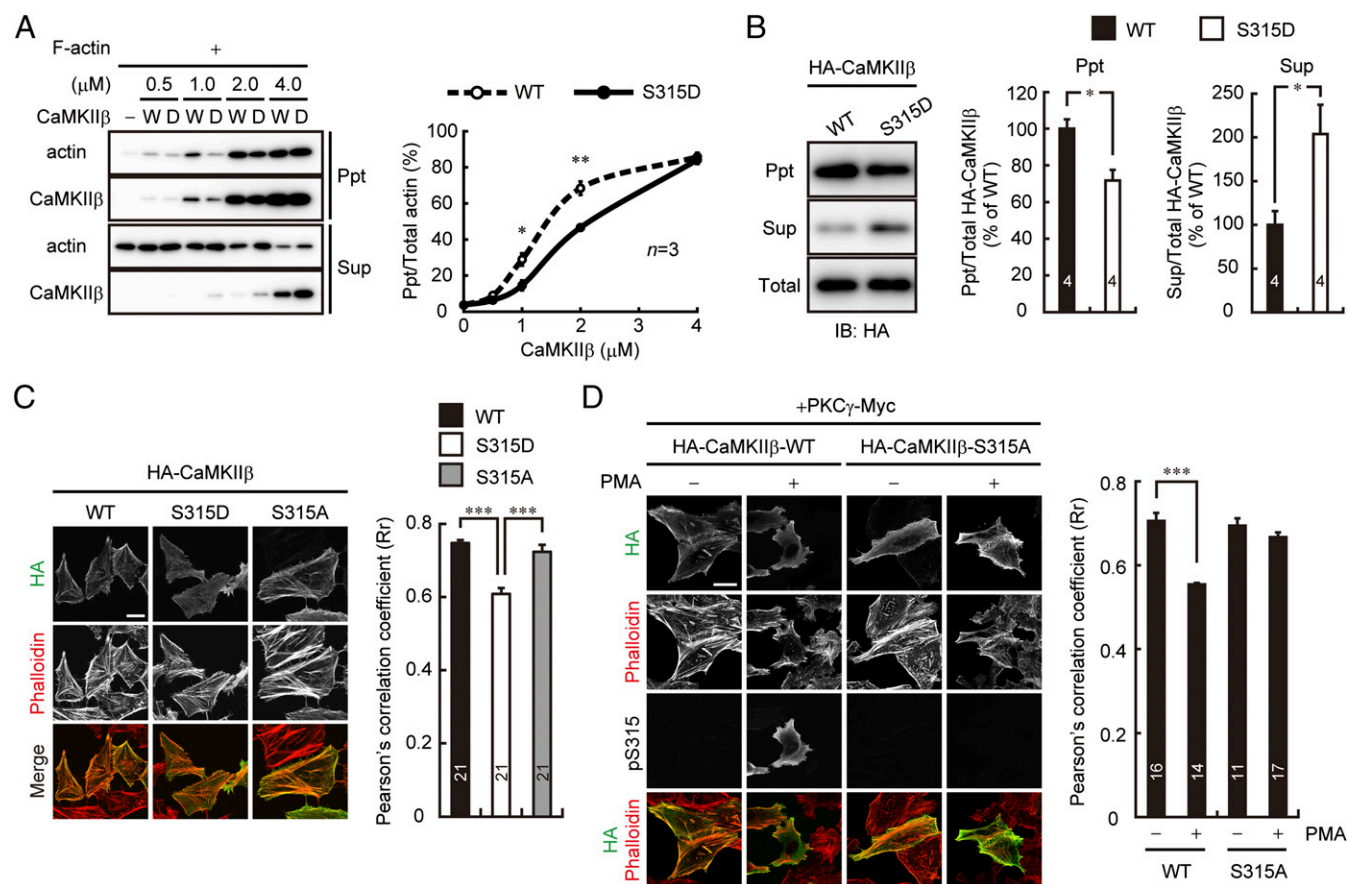


Fig. 5. Phosphorylation of CaMKII β at S315 attenuates its F-actin binding and bundling activity. (A) In vitro F-actin sedimentation assay with various amount of WT (W) or S315D (D) mutant form of CaMKII β . The supernatant (Sup) and pellet (Ppt) were probed with the indicated antibodies. Percentage of the bundled F-actin at various concentrations of CaMKII β were plotted (Right). * $P < 0.05$, ** $P < 0.01$, Student's t test for each concentration of CaMKII β . (B) Detection of HA-CaMKII β in the supernatant (Sup) and actin-rich pellet (Ppt) fractions of HeLa cells by detergent-extraction protocol. Right shows relative amount of HA-CaMKII β in each of the fractions as the percentage of WT. * $P < 0.05$, Student's t test. (C) Immunostaining of HA-CaMKII β -WT, S315D, or S315A in HeLa cells. F-actin was visualized with phalloidin-594. (Scale bar, 20 μ m.) Right shows quantification of colocalization of HA-CaMKII β with F-actin by the Pearson's correlation coefficient (Rr). *** $P < 0.0001$, one-way ANOVA with Bonferroni's test for multiple comparisons. (D) Immunostaining of HA-CaMKII β -WT or S315A cotransfected with PKC γ -Myc in HeLa cells. The transfected cells were treated (+) or not treated (-) with 100 nM PMA for 30 min, stained with indicated antibodies, and analyzed as in C. *** $P < 0.0001$, Mann-Whitney U test (WT); $P = 0.181$, Student's t test (S315A). (Scale bar, 30 μ m.) The numbers of experiments (A and B) or cells (C and D) are indicated in each graph.

causes spine abnormalities of Purkinje cells in *L7-Cre;Itpr1^{lox/lox}* mice. To test this hypothesis, we tried to correct the spine abnormalities in *L7-Cre;Itpr1^{lox/lox}* Purkinje cells by inhibiting the CaMKII β /F-actin interaction. KN-93, a potent inhibitor for CaMKII, has been shown to inhibit not only kinase activity but also F-actin interaction with CaMKII β (35, 36). Indeed, we confirmed that treatment with KN-93, but not an inactive analog KN-92, induced dissociation of HA-CaMKII β -S315A from F-actin in HeLa cells (Fig. S6).

To inhibit the CaMKII β /F-actin interaction in *L7-Cre;Itpr1^{lox/lox}* Purkinje cells in vivo, we chronically perfused KN-93 into the mouse cerebella for a week by means of an osmotic pump. Strikingly, spine density and length of KN-93-treated *L7-Cre;Itpr1^{lox/lox};Pcp2-GFP* Purkinje cells became equivalent to those of *Itpr1^{lox/lox};Pcp2-GFP* Purkinje cells treated with KN-92 or KN-93 (Fig. 7A and B). KN-93 did not significantly affect spine morphology in control *Itpr1^{lox/lox};Pcp2-GFP* Purkinje cells, suggesting that the phosphorylation of S315-CaMKII β interferes with its F-actin bundling and suppresses the excess spine formation and elongation in Purkinje cells. These results strongly suggested that the excess bundling of F-actin by CaMKII β due to the lack of S315 phosphorylation underlies abnormally numerous and elongated spines in IP $_3$ R1-deficient Purkinje cells in vivo. In KN-93-treated *L7-Cre;Itpr1^{lox/lox};Pcp2-GFP* Purkinje cells, we observed a slightly decreased width of spine heads

(Fig. 7B), but the reason was unclear and might be due to its off-target effects (37, 38).

Discussion

In this study, we identified a previously unknown mechanism in which PKC-mediated phosphorylation of CaMKII β maintains the appropriate spine density and morphology of Purkinje cells along distal dendrites. We found that CaMKII β increases spine density and length in Purkinje cells through its F-actin bundling activity. The spine increase and elongation depends on the CaMKII β phosphorylation state at S315, because the phosphorylation interferes with F-actin cross-linking activity of CaMKII β . Ca $^{2+}$ -dependent isoforms of PKC phosphorylates CaMKII β at S315 under control of mGluR1 signaling. In addition, we showed that the phosphorylation of CaMKII β by PKC is impaired in IP $_3$ R1-deficient Purkinje cells that exhibit aberrant increase in spine density and length, and that the spine abnormalities are attenuated by pharmacological inhibition of CaMKII β /F-actin interaction. Based on these findings, we propose a model that CaMKII β regulates mature Purkinje cell spine morphologies by F-actin bundling, which is controlled by the S315 phosphorylation status of CaMKII β via mGluR1/IP $_3$ R1/PKC signaling. Our findings provide a framework for maintaining proper spine density and morphology in Purkinje cells for cerebellar functions.

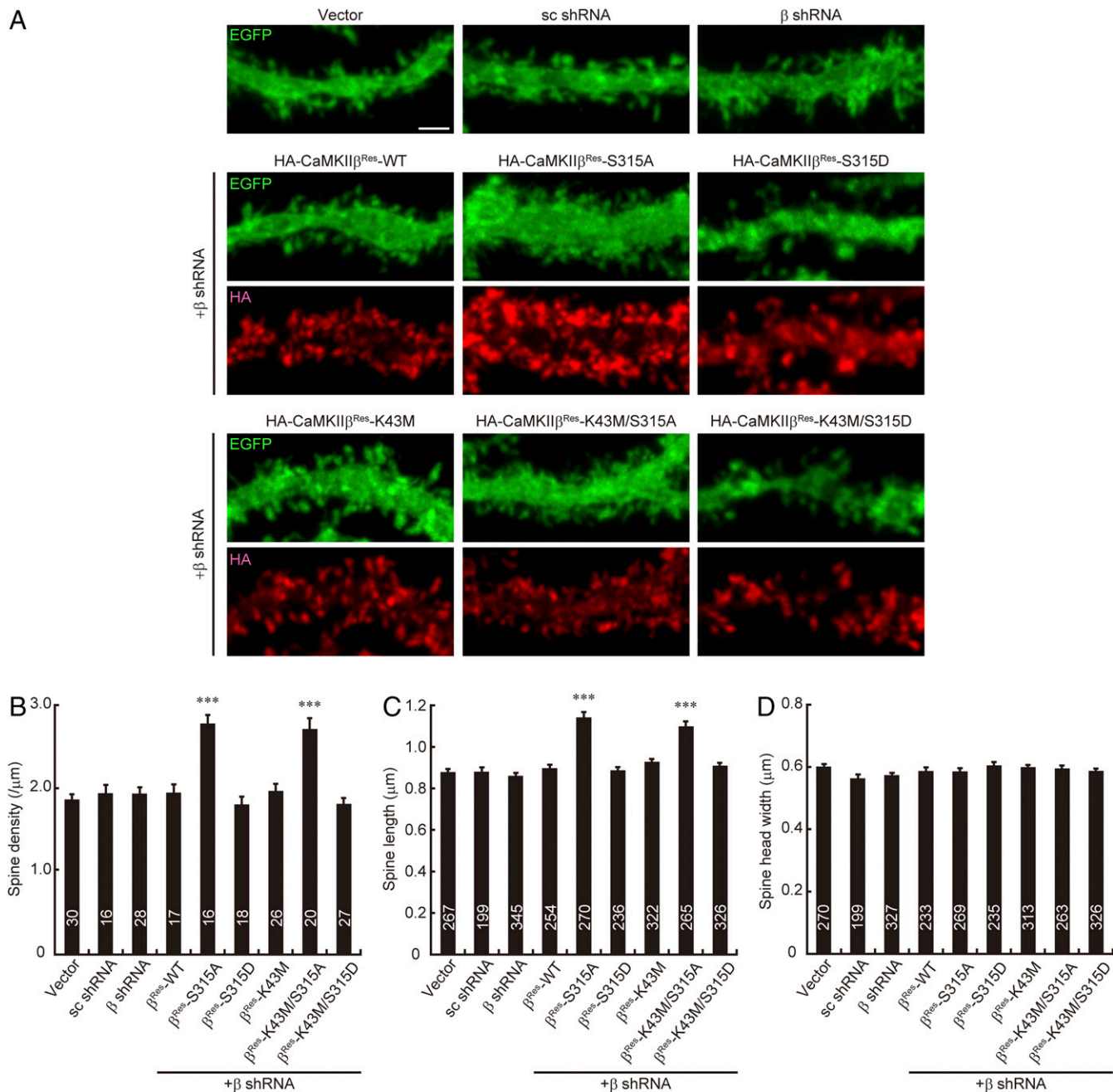


Fig. 6. Phosphorylation of CaMKII β at S315 regulates spine morphology of Purkinje cells. (A) Effects of phosphorylation state of CaMKII β at S315 on Purkinje cell dendritic spine morphology in cerebellar slice cultures. Cerebellar slices were subjected to biolistic transfection with the indicated plasmids, cultured for 4 d, and immunostained with anti-GFP (green) and HA (red) antibodies. Representative images of distal dendrites of Purkinje cells are shown. (Scale bar, 2 μm .) (B–D) Quantitative analysis of spine density (B), spine length (C), and spine head width (D) along the distal dendrites of EGFP⁺ Purkinje cells in A. *** $P < 0.0001$, one-way ANOVA with Dunnett's multiple-comparison post hoc test compared with vector control. The numbers of neurons (B) or spines (C and D) are indicated in each graph.

Purkinje cell dendrites are characterized by two compartments, the proximal and the distal dendritic regions, and spinogenesis at each dendritic compartment is controlled by different mechanisms during development. The proximal dendritic regions are innervated by climbing fibers, and spinogenesis on these proximal branches is inhibited by synaptic inputs from climbing fibers (39). On the other hand, distal dendritic regions have numerous spines, which are innervated by parallel fibers through the glutamate receptor delta2 (GluR δ 2)–Cbln1–neurexin mechanism (40–42). Several molecules have also been identified as regulators for the spinogenesis in Purkinje cells during development. For instance, retinoic-acid orphan

receptor alpha (ROR α) and β -III spectrin, which is implicated as a transcriptional target of ROR α , are critical for Purkinje cell spine development (43–46). In contrast to medical science's accumulating knowledge of spine regulation during development, little is known about how spines on the distal branches are maintained in mature Purkinje cells in vivo. In this study, we have shown that spines of Purkinje cells are maintained by CaMKII β /F-actin bundling, and that synaptic activity can regulate the mechanism by PKC-mediated CaMKII β phosphorylation. In addition, we have shown that expression of CaMKII β -S315A, but not CaMKII β -S315D, increased spine density and length of Purkinje cells, and that the defect of

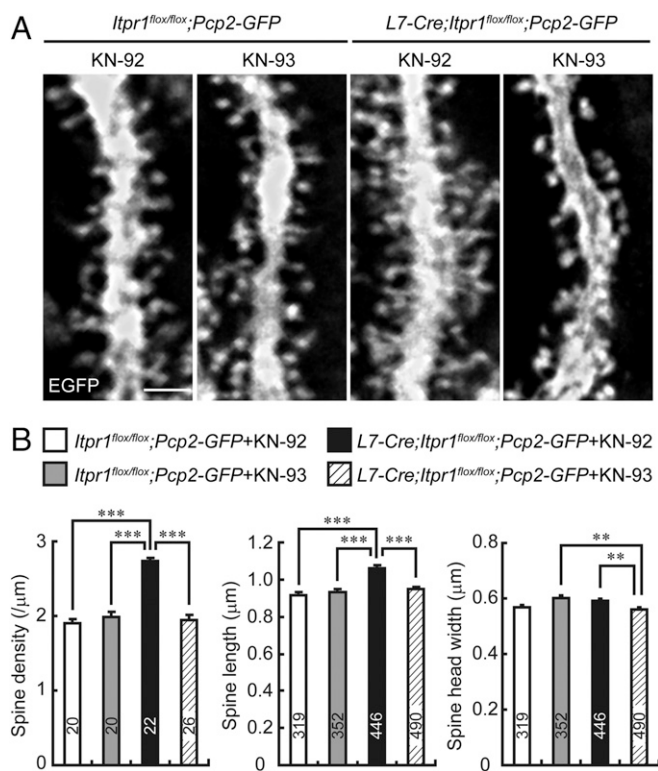


Fig. 7. Chronic inhibition of interaction between CaMKII β and F-actin ameliorates spine abnormalities of Purkinje cells in adult *L7-Cre;Itpr1^{flox/flox}* mice in vivo. (A) Spine morphology on distal dendrites of Purkinje cells from *Itpr1^{flox/flox};Pcp2-GFP* or *L7-Cre;Itpr1^{flox/flox};Pcp2-GFP* mice treated with KN-93 or KN-92. Sagittal cerebellar sections were stained with anti-GFP antibody. (Scale bar, 2 μ m.) (B) Quantitative analysis of spine density (Left), spine length (Center), and spine head width (Right) of distal dendrites of Purkinje cells. $^{***}P < 0.001$, $^{**}P < 0.0001$, one-way ANOVA with Bonferroni's test for multiple comparison. White bars: KN-92-treated *Itpr1^{flox/flox};Pcp2-GFP* Purkinje cells. Gray bars: KN-93 treated *Itpr1^{flox/flox};Pcp2-GFP* Purkinje cells. Black bars: KN-92 treated *L7-Cre;Itpr1^{flox/flox};Pcp2-GFP* Purkinje cells. Hatched bars: KN-93 treated *L7-Cre;Itpr1^{flox/flox};Pcp2-GFP* Purkinje cells. The numbers of neurons or spines are indicated in each graph.

S315 phosphorylation of CaMKII β underlies the abnormal spines at the distal dendritic region of mature Purkinje cells in IP₃R1-deficient mice (26). Thus, phosphorylation of S315-CaMKII β by PKC via mGluR/IP₃R1 signaling is a critical regulator of the CaMKII β /F-actin interaction, and the mechanism contributes to the suppression of excess spine formation and elongation, particularly in distal branches of mature Purkinje cells. Because PKC is basically activated in Purkinje cells (47), it is possible that mGluR is tonically activated under basal condition and constantly induces S315 phosphorylation of CaMKII β through the mGluR/IP₃R1/PKC signaling pathway, which would maintain a balance between the CaMKII β /F-actin-mediated spinogenesis and its repression. Although further study is necessary, such a delicate balance of the phosphorylation-dependent regulation might, at least in part, explain why Purkinje cells lacking CaMKII β exhibit no apparent spine abnormalities (20, 34).

Whereas a close link between spine structural rearrangement caused by synaptic plasticity and learning/memory has been thoroughly studied, particularly in cortical and hippocampal neurons (48, 49), a previous study has suggested that spine morphology on distal branches of Purkinje cells is not affected by induction of parallel fiber–Purkinje cell LTD (50). However, recent studies have also demonstrated that cerebellar motor learning decreases spine density in Purkinje cells (8, 9). Although a molecular mechanism of spine plasticity in Purkinje cells associated with long-term motor

learning is unknown, our findings, at least in part, could provide a potential molecular mechanism that links synaptic inputs to spine structural plasticity in Purkinje cells. Because both the activity-dependent CaMKII β phosphorylation revealed by the present study and LTD in parallel fiber–Purkinje cell synapse share the mGluR1/IP₃R1/PKC signaling pathway (51), the phosphorylated form of CaMKII β at S315 might also contribute to parallel fiber–Purkinje cell synaptic transmission in a different manner. Because actin polymerization is important for GluR2 subunit endocytosis and both basal PKC and MEK/ERK1/2 activities contribute to AMPARs internalization (47), CaMKII β -mediated F-actin bundling and its regulation by PKC-mediated phosphorylation may also contribute to AMPARs internalization during LTD by controlling endocytosis.

In summary, we demonstrated a previously unknown regulatory mechanism of distal dendritic spinogenesis in mature Purkinje cells, which is dependent on both CaMKII β /F-actin interaction and mGluR/IP₃R1/PKC signaling. A recent study has reported that in hippocampal neurons, autophosphorylation within the F-actin binding region of CaMKII β following through NMDA receptor-mediated Ca²⁺ influx regulates its function as a regulator of F-actin dynamics during synaptic plasticity (18). On the contrary, our study demonstrated that in Purkinje cells, PKC-mediated phosphorylation of CaMKII β regulates its F-actin bundling under mGluR/IP₃R1 signaling, which represses unnecessary spine development. In the absence of the mechanism, Purkinje cells would have wrong wiring, which causes extremely severe ataxia like IP₃R1-deficient mice (26). Therefore, the mechanism would be an important mechanism for maintaining proper cerebellar circuits to express cerebellar functions in vivo.

Materials and Methods

Animals. *Itpr1^{-/-}*, *L7-Cre;Itpr1^{flox/flox}*, and *L7-Cre;Itpr1^{flox/flox};Pcp2-GFP* mice were used as previously reported (26, 52). ICR mice were purchased from Japan SLC, Inc. Mice were bred in a pathogen-free environment with a 12-h light–dark cycle. Japanese white rabbits were purchased from Oriental Yeast Co., Ltd. All animal experiments were performed in accordance with the guidelines approved by the Animal Experiments Committee of RIKEN Brain Science Institute. Both female and male mice were included in the analysis.

Antibodies. For production of a phospho-specific antibody for CaMKII β phosphorylated at S315 (pS315-CaMKII β), BSA-conjugated synthetic phospho-peptide (C-LATRNFPVSGRQTTA, corresponding to residues 309–322) was injected into female Japanese white rabbits. The phospho-specific antibody was purified by affinity chromatography on the phospho-peptide coupled-Sepharose, and nonphospho-specific antibodies were subsequently absorbed with nonphospho-peptide unphosphorylated CaMKII β (C-LATRNFPVSGRQTTA) and phospho-peptide pS314-CaMKII α (C-LATRNFPVSGKSGGN, corresponding to residues 308–321)-coupled Sepharose. Rabbit polyclonal anti-calbindin (CB38, Swant), guinea pig polyclonal anti-calbindin (GP-Af280, Frontier Institute), mouse monoclonal anti-GFP (clone 1E4, M048-3, MBL), rabbit polyclonal anti-GFP (632592, Clontech), mouse monoclonal anti-CaMKII β (clone CB- β 1, 13–9800, Zymed), rabbit polyclonal anti-phospho T286-CaMKII (ab5683, Abcam), mouse monoclonal anti- β -actin (clone AC-15, A5441, Sigma), guinea pig polyclonal anti-PKC γ (GP-Af350, Frontier Institute), rat monoclonal anti-HA (clone 3F10, 11867423001, Roche), mouse monoclonal anti-c-myc (clone 9E10, sc-40, Santa cruz), rabbit polyclonal anti-phospho (Ser152/156) MARCKS (07-1238, Millipore), mouse monoclonal anti-MARCKS (clone 2C2, WH0004082M6, Sigma), and mouse monoclonal anti-GST (clone B-14, sc-138, Santa cruz) antibodies were purchased.

Plasmids. The cDNA encoding mouse CaMKII β was obtained from the RIKEN FANTOM cDNA library (clone ID B930031B11) (53) and amplified by PCR using the primers 5'-ATAAGCTTATGGCCACCACGGTGACC-3' and 5'-TAGAATTCTC-CTGCAGTGGGGCCAC-3' (the underlined regions indicate HindIII and EcoRI sites, respectively). The PCR product was cloned into the mammalian expression vector pcDNA3.1 (Invitrogen) or insect cell expression vector pFastBac1 (Life Technologies). K43M, S315A, and S315D mutants of CaMKII β were generated by site-directed mutagenesis with KOD Plus DNA polymerase (TOYOBO). GST-CaMKII β (272–407 aa) was constructed by using PCR with primers 5'-TAA-GAATTCTGCTGCCAACGATCCACGG-3' and 5'-GGCGAATTCTCAGGCATCTCGT-CCTCTATG-3' (the underlined regions indicate the EcoRI restriction site) and cloned into pGEX-4T-1 (Pharmacia). The cDNA encoding mouse PKC γ was

amplified by RT-PCR from adult mouse cerebellum cDNA using the primers 5'-TAAGTGACCATGCGGGTCTGGCCCTGGCGGAGCGAC-3' and 5'-GATGGT-ACCTTACATGACAGGCACGGGCACAGGGCTTG-3' (the underlined regions indicate the KpnI restriction site) and cloned into pCDNA3.1 or pFastBac1.

For CaMKII β knockdown, we used 5'-GAGTATGCAGCAAGATCA-3' as an shRNA target sequence of mouse CaMKII β and 5'-GGCTTACAGATCGAAACA-3' as a control scramble shRNA. The shRNA sequences were subcloned into a plasmid-based expression vector, pSUPER (OligoEngine). The mEGFP (monomeric EGFP with A206K mutation) gene was also cloned into the pSUPER vector downstream of the PGK promoter. The shRNA-resistant form of CaMKII β (indicated as β^{res}) was generated by introducing silent mutations at the shRNA target region with site-directed mutagenesis. pEGFP-C1 was purchased (Clontech). All constructed plasmids were verified by DNA sequencing.

Cell Culture, Transfection, and Immunocytochemistry. HeLa cells were cultured in Dulbecco's modified essential medium (DMEM) containing 10% (vol/vol) FBS, 50 units/mL penicillin, and 50 μ g/mL streptomycin. HA-CaMKII β and PKC γ -flag or -Myc were transfected in HeLa cells using FuGENE HD transfection reagent (Promega). At 1 d after transfection, cells were incubated in balanced-salt solution (BSS) (20 mM Hepes, pH 7.4, 115 mM NaCl, 5.4 mM KCl, 2 mM CaCl₂, 1 mM MgCl₂, and 10 mM glucose) for 2 h. Cells were then treated with 100 nM PMA (Enzo Life Sciences) for 30 min or with 1 μ M okadaic acid (Calbiochem) for 30 min. The treated cells were fixed with 4.0% paraformaldehyde (PFA) in PBS for 10 min at room temperature. After being washed with PBS, cells were permeabilized with 0.2% Triton-X 100 in PBS for 5 min. The coverslips were blocked with 1.0% BSA or skimmed milk and 1.0% normal goat serum (NGS) in PBS for 60 min at room temperature, and then, incubated with the primary antibodies overnight at 4 °C. After being washed with PBS, the coverslips were incubated with Alexa Fluor 488-, 594-conjugated (Invitrogen) and Cy5-conjugated secondary antibodies (Jackson ImmunoResearch) and Alexa Fluor 594-conjugated phalloidin (Invitrogen) for 1 h at room temperature. After being washed with PBS, the coverslips were mounted with Vectashield (Vector Laboratories). The primary antibodies were anti-pS315-CaMKII β (2 μ g/mL), anti-HA (1:500), and anti-PKC γ (1:250).

Cerebellar Primary Culture. Cerebellar primary cultures were prepared basically as described previously (54). Briefly, cerebella were dissected from postnatal day 1 ICR, C57/BL6 *Itp1^{+/+}*, or *Itp1^{-/-}* mice. Cerebellar cells were suspended in serum-free medium at a density of 4×10^6 cells per milliliter. Eighty microliters of the suspension was spotted onto plastic coverslips (13.5 mm in diameter; Sumilon, Sumitomo Bakelite), coated with 100 μ g/mL poly-L-lysine, and placed in a humidified CO₂ incubator (5.0% CO₂ at 37 °C). After 3 h, medium was added to each well. The medium was composed of Eagle's MEM supplemented with 1.0 mg/mL BSA (Sigma), 1.0 mg/mL insulin-transferrin-serenium (Invitrogen), 0.1 nM L-tyroxine (T4) (Sigma), 1.0 μ g/mL aprotinin (Sigma), 0.25% glucose, 2.0 mM glutamine, 2.0 mg/mL Na₂CO₃, 100 units/mL penicillin, and 135 μ g/mL streptomycin. Cultures were used at 21–27 d in vitro (DIV). To monitor the level of pS315-CaMKII β , cells were incubated in Hepes-buffered saline (HBS) (20 mM Hepes, pH 7.4, 135 mM NaCl, 4 mM KCl, 1 mM Na₂HPO₄, 2 mM CaCl₂, 1 mM MgCl₂, 10 mM glucose) in the presence or absence of Go6976 (Calbiochem) for 2 h. Cells were then treated with glutamate, DHPG (Tocris), AMPA (Tocris), PMA, or HBS containing 55 mM KCl and 84 mM NaCl (high K⁺). The treated cells were fixed with 4% PFA and immunostained. The primary antibodies were anti-pS315-CaMKII β (5 μ g/mL), anti-CaMKII β (1:500), and guinea pig anti-calbindin (1:250).

Acute Cerebellar Slice. Two- to three-month-old *IP₃R1^{fllox/fllox}* or *L7-Cre;IP₃R1^{fllox/fllox}* mice were used. Under pentobarbital anesthesia, mice were transcardially perfused with ice-cold cutting solution containing 120 mM choline Cl, 3 mM KCl, 8 mM MgCl₂, 1.25 mM NaH₂PO₄, 10 mM glucose, and 26 mM NaHCO₃, and the cerebella was excised. Sagittal cerebellar slices (250- μ m thickness) were prepared from the vermis using a Vibratome-type tissue slicer (Leica VT1000S, Leica Microsystems). The slices were kept at 32 °C for 1.5–2 h in artificial CSF (ACSF) containing 124 mM NaCl, 2.5 mM KCl, 2 mM CaCl₂, 2 mM MgSO₄, 1.25 mM NaH₂PO₄, 20 mM glucose, and 26 mM NaHCO₃, equilibrated with 95% O₂ and 5% CO₂, and were then treated with 100 μ M DHPG or 0.4 μ M PMA at 32 °C. The treated slices were fixed with 4% PFA for 3 h and immersed in 30% sucrose in PBS overnight at 4 °C. The slices were resectioned on the

sagittal plane at 12- μ m thickness with a cryostat (HM550, MICROM), and the sections were subjected to immunohistochemistry.

Cerebellar Slice Culture and Biolistic Transfection. Cerebellar slice culture and biolistic transfection using a Helios gene gun were performed as described previously (55). ICR mice, 14 to 17 d old, were used. Two or 4 d after transfection, slices were fixed with 4% PFA, permeabilized, and immunostained with polyclonal anti-GFP (1:500) and anti-HA (1:500).

Immunohistochemistry. For immunohistochemistry of cerebellar sections, mice were deeply anesthetized with pentobarbital and transcardially perfused with saline and 0.1 M phosphate buffer (PB) containing 4% PFA. The brains were dissected out, and then postfixed in PFA at 4 °C for 3 h, and immersed in 30% sucrose in PB overnight at 4 °C. The brains were sectioned sagittally at 12- μ m thickness with a cryostat or at 30- μ m thickness with a Vibratome-type tissue slicer. Cerebellar sections were processed as described previously (26). The primary antibodies used were pS315-CaMKII β (5 μ g/mL), anti-CaMKII β (1:500), guinea pig polyclonal anti-calbindin (1:250), rabbit polyclonal anti-calbindin (1:2,000), anti-phospho-MARCKS (1:400), anti-MARCKS (1:400), monoclonal anti-GFP (1:500), polyclonal anti-GFP (1:500), and anti-PKC γ (1:250).

Fluorescent Image Analysis. Fluorescent image acquisition by confocal laser microscope and spine analysis were performed as described previously (26). Colocalization analysis and fluorescence intensity analysis were performed using ImageJ software.

Immunoblotting. Transfected HeLa cells were lysed with TNE buffer containing 10 mM Tris-HCl, pH 7.5, 150 mM NaCl, 1 mM EDTA, 1 mM EGTA, 1% Nonidet P-40, 10 mM sodium pyrophosphate, 50 mM sodium fluoride, 1 mM sodium orthovanadate and protease inhibitor mixture, and cleared by centrifugation at 20,000 \times g for 15 min. The supernatants were subjected to SDS/PAGE. For cell fractionation, transfected HeLa cells were incubated in BSS for 2 h and homogenated in buffer containing 5 mM Hepes, pH 7.4, 0.32 M sucrose, 2 mM EDTA, 1 mM EGTA, 50 mM KCl, 1 mM 2-ME, 10 mM sodium pyrophosphate, 50 mM sodium fluoride, 1 mM sodium orthovanadate, and protease inhibitor mixture (Roche). The homogenate was centrifuged at 2,000 \times g for 10 min. Triton X-100 was added to the supernatant at a final 0.1% concentration, which was incubated at 4 °C for 30 min and was then centrifuged at 10,000 \times g for 30 min. The detergent-soluble (supernatant) and -insoluble (pellet) fractions were obtained and subjected to SDS/PAGE. The separated proteins by SDS/PAGE were transferred onto polyvinylidene difluoride membrane (Millipore). The membrane was blocked with 5% skimmed milk or BSA and 1% NGS in PBST (PBS containing 0.05% Tween 20) and then, incubated with the primary antibodies for 1 h at room temperature or overnight at 4 °C. After being washed with PBST, the membrane was incubated with horseradish peroxidase-conjugated secondary antibody (1:5,000; GE Healthcare) for 1 h at room temperature. The blot was developed using chemiluminescence reagents (Immobilion Western Chemiluminescent HRP Substrate, Millipore), and detected using an image analyzer (LAS-4000 mini, Fujifilm). For quantitative analysis, band intensities were quantified using ImageJ software. The primary antibodies were pS315-CaMKII β (1 μ g/mL), anti-phospho T286-CaMKII (1:1,000), anti-GST (1:200), anti-HA (1:1,000), anti-Myc (1:200), anti- β -actin (1:5,000), and anti-CaMKII β (1:1,000).

Statistical Analysis. All data are shown as means \pm SEM, and statistical significance was determined as indicated in the figure legends.

More details of the materials and methods are in *SI Materials and Methods*.

ACKNOWLEDGMENTS. We thank all members of our laboratory, especially Dr. K. Kawai and Dr. M. W. Sherwood, for valuable discussion and support; all staff members of the Brain Science Institute (BSI) Research Resources Center Support Unit for Bio-Material Analysis for DNA sequencing and peptide synthesis, especially Mr. M. Usui's contribution to phosphopeptide mapping; Ms. S. Fukushima for antibody production; the BSI Research Resources Center Support Unit for Animal Resources Development for their assistance with animal care; and the Functional Annotation of Mouse (FANTOM) consortium for providing us the FANTOM clones. This work was supported by grants from RIKEN BSI and the Moritani Scholarship Foundation (to T.S. and to C.H.) and by the Japan Society for the Promotion of Science's Grants-in-Aid for Scientific Research 26830051 (to T.S.), 15K06761 (to C.H.), and 20220007 (to K.M.).

- Ito M (2006) Cerebellar circuitry as a neuronal machine. *Prog Neurobiol* 78:272–303.
- Jörnntell H, Hansel C (2006) Synaptic memories upside down: Bidirectional plasticity at cerebellar parallel fiber-Purkinje cell synapses. *Neuron* 52:227–238.
- Dunaevsky A, Tashiro A, Majewska A, Mason C, Yuste R (1999) Developmental regulation of spine motility in the mammalian central nervous system. *Proc Natl Acad Sci USA* 96:13438–13443.

- Velázquez-Zamora DA, Martínez-Degollado M, González-Burgos I (2011) Morphological development of dendritic spines on rat cerebellar Purkinje cells. *Int J Dev Neurosci* 29:515–520.
- Fiala JC, Spacek J, Harris KM (2002) Dendritic spine pathology: Cause or consequence of neurological disorders? *Brain Res Brain Res Rev* 39:29–54.
- Lee KJ, Kim H, Rhyu IJ (2005) The roles of dendritic spine shapes in Purkinje cells. *Cerebellum* 4:97–104.

7. Tsai PT, et al. (2012) Autistic-like behaviour and cerebellar dysfunction in Purkinje cell Tsc1 mutant mice. *Nature* 488:647–651.
8. Aziz W, et al. (2014) Distinct kinetics of synaptic structural plasticity, memory formation, and memory decay in massed and spaced learning. *Proc Natl Acad Sci USA* 111:E194–E202.
9. Wang W, et al. (2014) Distinct cerebellar engrams in short-term and long-term motor learning. *Proc Natl Acad Sci USA* 111:E188–E193.
10. Hlushchenko I, Koskinen M, Hotulainen P (2016) Dendritic spine actin dynamics in neuronal maturation and synaptic plasticity. *Cytoskeleton* 73:435–441.
11. Matus A (2000) Actin-based plasticity in dendritic spines. *Science* 290:754–758.
12. Hotulainen P, Hoogenraad CC (2010) Actin in dendritic spines: Connecting dynamics to function. *J Cell Biol* 189:619–629.
13. Erondy NE, Kennedy MB (1985) Regional distribution of type II Ca²⁺/calmodulin-dependent protein kinase in rat brain. *J Neurosci* 5:3270–3277.
14. Bayer KU, Schulman H (2001) Regulation of signal transduction by protein targeting: The case for CaMKII. *Biochem Biophys Res Commun* 289:917–923.
15. Fink CC, et al. (2003) Selective regulation of neurite extension and synapse formation by the beta but not the alpha isoform of CaMKII. *Neuron* 39:283–297.
16. Thiagarajan TC, Piedras-Renteria ES, Tsien RW (2002) alpha- and betaCaMKII. Inverse regulation by neuronal activity and opposing effects on synaptic strength. *Neuron* 36:1103–1114.
17. Okamoto K, Narayanan R, Lee SH, Murata K, Hayashi Y (2007) The role of CaMKII as an F-actin-bundling protein crucial for maintenance of dendritic spine structure. *Proc Natl Acad Sci USA* 104:6418–6423.
18. Kim K, et al. (2015) A temporary gating of actin remodeling during synaptic plasticity consists of the interplay between the kinase and structural functions of CaMKII. *Neuron* 87:813–826.
19. Miller SG, Kennedy MB (1985) Distinct forebrain and cerebellar isozymes of type II Ca²⁺/calmodulin-dependent protein kinase associate differently with the post-synaptic density fraction. *J Biol Chem* 260:9039–9046.
20. Nagasaki N, Hirano T, Kawaguchi SY (2014) Opposite regulation of inhibitory synaptic plasticity by α and β subunits of Ca(2+)/calmodulin-dependent protein kinase II. *J Physiol* 592:4891–4909.
21. Hansel C, et al. (2006) alphaCaMKII is essential for cerebellar LTD and motor learning. *Neuron* 51:835–843.
22. Walaas SI, et al. (1988) Cell-specific localization of the alpha-subunit of calcium/calmodulin-dependent protein kinase II in Purkinje cells in rodent cerebellum. *Brain Res* 464:233–242.
23. O'Leary H, Lasda E, Bayer KU (2006) CaMKIIbeta association with the actin cytoskeleton is regulated by alternative splicing. *Mol Biol Cell* 17:4656–4665.
24. Mizutani A, Kuroda Y, Futatsugi A, Furuichi T, Mikoshiba K (2008) Phosphorylation of Homer3 by calcium/calmodulin-dependent kinase II regulates a coupling state of its target molecules in Purkinje cells. *J Neurosci* 28:5369–5382.
25. Kano M, Hashimoto K, Tabata T (2008) Type-1 metabotropic glutamate receptor in cerebellar Purkinje cells: A key molecule responsible for long-term depression, endocannabinoid signalling and synapse elimination. *Philos Trans R Soc Lond B Biol Sci* 363:2173–2186.
26. Sugawara T, et al. (2013) Type 1 inositol trisphosphate receptor regulates cerebellar circuits by maintaining the spine morphology of purkinje cells in adult mice. *J Neurosci* 33:12186–12196.
27. Ito M (2002) The molecular organization of cerebellar long-term depression. *Nat Rev Neurosci* 3:896–902.
28. Martiny-Baron G, et al. (1993) Selective inhibition of protein kinase C isozymes by the indolocarbazole Gö 6976. *J Biol Chem* 268:9194–9197.
29. Saito N, Kikkawa U, Nishizuka Y, Tanaka C (1988) Distribution of protein kinase C-like immunoreactive neurons in rat brain. *J Neurosci* 8:369–382.
30. Heemskerk FM, Chen HC, Huang FL (1993) Protein kinase C phosphorylates Ser152, Ser156 and Ser163 but not Ser160 of MARCKS in rat brain. *Biochem Biophys Res Commun* 190:236–241.
31. Ramsden JJ (2000) MARCKS: A case of molecular exaptation? *Int J Biochem Cell Biol* 32:475–479.
32. Egelhoff TT, Brown SS, Spudich JA (1991) Spatial and temporal control of nonmuscle myosin localization: Identification of a domain that is necessary for myosin filament disassembly in vivo. *J Cell Biol* 112:677–688.
33. Shen K, Teruel MN, Subramanian K, Meyer T (1998) CaMKIIbeta functions as an F-actin targeting module that localizes CaMKIIalpha/beta heterooligomers to dendritic spines. *Neuron* 21:593–606.
34. van Woerden GM, et al. (2009) betaCaMKII controls the direction of plasticity at parallel fiber-Purkinje cell synapses. *Nat Neurosci* 12:823–825.
35. Lin YC, Redmond L (2008) CaMKIIbeta binding to stable F-actin in vivo regulates F-actin filament stability. *Proc Natl Acad Sci USA* 105:15791–15796.
36. Waggenger CT, Dupree JL, Elgersma Y, Fuss B (2013) CaMKII β regulates oligodendrocyte maturation and CNS myelination. *J Neurosci* 33:10453–10458.
37. Hidaka H, Yokokura H (1996) Molecular and cellular pharmacology of a calcium/calmodulin-dependent protein kinase II (CaM kinase II) inhibitor, KN-62, and proposal of CaM kinase phosphorylation cascades. *Adv Pharmacol* 36:193–219.
38. Hook SS, Means AR (2001) Ca(2+)/CaM-dependent kinases: From activation to function. *Annu Rev Pharmacol Toxicol* 41:471–505.
39. Cesa R, Strata P (2005) Axonal and synaptic remodeling in the mature cerebellar cortex. *Prog Brain Res* 148:45–56.
40. ELEGHEERT J, et al. (2016) Structural basis for integration of GluD receptors within synaptic organizer complexes. *Science* 353:295–299.
41. Matsuda K, et al. (2010) Cbln1 is a ligand for an orphan glutamate receptor delta2, a bidirectional synapse organizer. *Science* 328:363–368.
42. Uemura T, et al. (2010) Trans-synaptic interaction of GluRdelta2 and Neurexin through Cbln1 mediates synapse formation in the cerebellum. *Cell* 141:1068–1079.
43. Gao Y, et al. (2011) β -III spectrin is critical for development of purkinje cell dendritic tree and spine morphogenesis. *J Neurosci* 31:16581–16590.
44. Gold DA, et al. (2003) RORalpha coordinates reciprocal signaling in cerebellar development through sonic hedgehog and calcium-dependent pathways. *Neuron* 40:1119–1131.
45. Gold DA, Gent PM, Hamilton BA (2007) ROR alpha in genetic control of cerebellum development: 50 staggering years. *Brain Res* 1140:19–25.
46. Takeo YH, Kakegawa W, Miura E, Yuzaki M (2015) ROR α regulates multiple aspects of dendrite development in cerebellar purkinje cells in vivo. *J Neurosci* 35:12518–12534.
47. Tatsukawa T, Chimura T, Miyakawa H, Yamaguchi K (2006) Involvement of basal protein kinase C and extracellular signal-regulated kinase 1/2 activities in constitutive internalization of AMPA receptors in cerebellar Purkinje cells. *J Neurosci* 26:4820–4825.
48. Fortin DA, Srivastava T, Soderling TR (2012) Structural modulation of dendritic spines during synaptic plasticity. *Neuroscientist* 18:326–341.
49. Kasai H, Fukuda M, Watanabe S, Hayashi-Takagi A, Noguchi J (2010) Structural dynamics of dendritic spines in memory and cognition. *Trends Neurosci* 33:121–129.
50. Sdrulla AD, Linden DJ (2007) Double dissociation between long-term depression and dendritic spine morphology in cerebellar Purkinje cells. *Nat Neurosci* 10:546–548.
51. Ito M, Yamaguchi K, Nagao S, Yamazaki T (2014) Long-term depression as a model of cerebellar plasticity. *Prog Brain Res* 210:1–30.
52. Matsumoto M, et al. (1996) Ataxia and epileptic seizures in mice lacking type 1 inositol 1,4,5-trisphosphate receptor. *Nature* 379:168–171.
53. Carninci P, et al.; FANTOM Consortium; RIKEN Genome Exploration Research Group and Genome Science Group (Genome Network Project Core Group) (2005) The transcriptional landscape of the mammalian genome. *Science* 309:1559–1563.
54. Hisatsune C, et al. (2006) Inositol 1,4,5-trisphosphate receptor type 1 in granule cells, not in Purkinje cells, regulates the dendritic morphology of Purkinje cells through brain-derived neurotrophic factor production. *J Neurosci* 26:10916–10924.
55. Fukatsu K, Bannai H, Inoue T, Mikoshiba K (2010) Lateral diffusion of inositol 1,4,5-trisphosphate receptor type 1 in Purkinje cells is regulated by calcium and actin filaments. *J Neurochem* 114:1720–1733.